Observations of Achernar with VINCI

Pierre Kervella

LESIA, UMR 8109, Observatoire de Paris-Meudon, 5, place Jules Janssen, 92195 Meudon, France

Abstract

The southern star Achernar is the brightest Be star, a class of massive and fast rotating stars. We describe here a pratical application of interferometry to the observation of this star, using the VINCI/VLTI instrument in the near-infrared domain. The fast rotation of Achernar distorts its photosphere, and a relatively dense stellar wind is created by the overheated poles of this star. The presence of these two components (elliptical photosphere and extended envelope) requires the use of moderately complex models to interpret interferometric visibilities.

Key words: Techniques: interferometric, Stars: emission-line, Be, Stars: rotation, Stars: individual: Achernar, Stars: circumstellar matter, Methods: data analysis
PACS: , 95.75.Kk, 97.10.-q, 97.10.Kc, 97.10.Fy

1. Why observe Achernar?

The southern star Achernar (α Eridani, HD 10144) is the brightest and one of the nearest of all Be stars ($m_V = 0.46$, $\pi = 22.7 \pm 0.6$ mas). Depending on the author (and the technique used) the spectral type of Achernar ranges from B3-B4IIIe to B4Ve (Slettebak, 1982; Balona, Engelbrecht & Marang, 1987). The estimated projected rotation velocity $v \sin i$ ranges from 220 to 270 km/s and the effective temperature $T_{\rm eff}$ from 15 000 to 20 000 K (Vinicius et al., 2006; Chauville et al., 2001). Such rapid rotation ($\geq 80\%$ of the critical velocity) induces two effects on the star structure: a rotational flattening and an equatorial darkening (von Zeipel, 1924).

Domiciano de Souza et al. (2003), hereafter D03, measured the apparent rotational flattening of Achernar using the Very Large Telescope Interferometer (VLTI). The data analysed by these authors are considered in the present paper, as well as additional VINCI data reported in Kervella & Domiciano de Souza (2006). They showed that the flattening

Email address: pierre.kervella@obspm.fr (Pierre Kervella).

ratio measured on this star cannot be explained in the Roche approximation, especially when taking the von Zeipel effect into account. Rapid rotation and gravity darkening seem to be important keys to explaining the two-component circumstellar environment (CSE) of Be stars: (1) a dense (particle densities $N \simeq 10^{11} - 10^{12}$ cm^{-3}), high mass-loss ($\simeq 10^{-8}$ M$_\odot$/yr) and low radial velocity ($\simeq 10 - 100$ km/s) equatorial envelope and (2) a rarefied ($N \simeq 10^{9}$ cm^{-3}), low mass-loss ($\simeq 10^{-10}$ M$_\odot$/yr) and fast ($\simeq 1000$ km/s) polar wind (Damineli Neto & de Freitas-Pacheco, 1982; Waters, Cote & Lamers, 1987). This picture of a two-component circumstellar envelope (CSE) is based on many observations performed in the past few decades.

The disk-like shape of the dense equatorial CSE has been directly measured by interferometric observations in the radio and optical/IR (Dougherty & Taylor, 1992; Stee et al., 1995; Quirrenbach et al., 1997). In a recent work, Tycner et al. (2005) explore the relationship between the angular size of the Hα emitting region (measured by interferometry) and the net Hα emission measured spectroscopically for seven Be stars. They find an interesting correlation between the two quantities, which they attribute to an optically thick emission proportional to the effective area of the emitting disk. Because the equatorial disks are denser ($\simeq 100$ times) than the polar winds and because the free-free emissivity is proportional to the density squared, the equatorial disk dominates the near-IR continuum emission when it is present.

However, it is still not clear if this free-free radiation comes only from the equatorial envelope or if it can also be formed, at least partially, in the polar wind. Modern high angular resolution techniques have the resolving power and sensitivity required to map the spatial distribution of the near-IR emission. In the present paper we summarize our investigations on this issue using the VINCI/VLTI near-IR instrument.

2. VINCI: a simple interferometric instrument

The VLT Interferometer Commissioning Instrument (VINCI, Fig. 1, left) is a two-telescopes beam combiner based on single-mode, fluoride glass fibers (Kervella et al., 2000, 2003). VINCI uses in general a regular K band filter ($\lambda = 2.0 - 2.4$ μm), but can also be operated in the H band ($\lambda = 1.4 - 1.8$ μm) using an integrated optics beam combiner (Berger et al., 2001; Lebouquin et al., 2004). Recently, the original K band beam combiner used for the observations of Achernar discussed here was replaced by an integrated optics device, also operating in the K band (Lebouquin et al., 2006). The basic principle of VINCI is to use single-mode waveguides to spatially filter and recombine the light collected by the two telescopes. Four outputs are produced: two photometric ones corresponding to each of the two telescopes, and two interferometric ones carrying the interference fringes in phase opposition. The efficiency of the injection of the stellar light in the two input fibers is monitored continuously using the two photometric outputs. These two signals are used in the data processing to normalize the fringe contrast. Fig. 1 (right) shows the principle of the MONA fibered beam combiner originally installed in VINCI and used for the observations of Achernar discussed in the present paper.

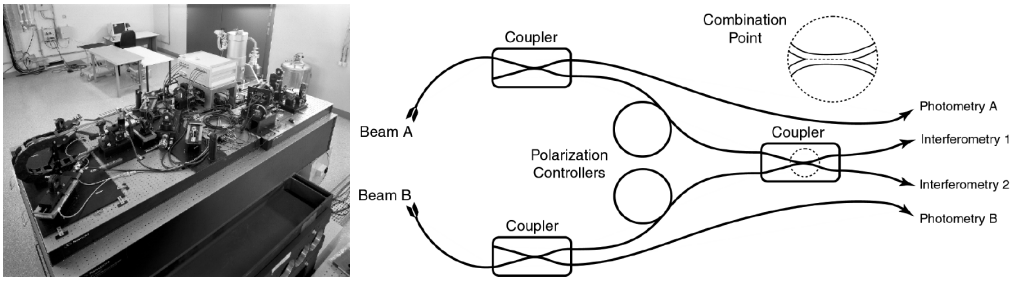

Fig. 1. *Left:* Photo of VINCI. *Right:* Principle of the MONA beam combiner.

3. Observations and data processing

Achernar was observed intensively using both the 0.35 m VLTI Test Siderostats and the 8 m Unit Telescopes. A total of nine VLTI baselines were used for this program, including five out of the six possible Unit Telescope baselines. Thanks to a very efficient supersynthesis effect, the coverage in azimuth of the projected baselines is almost complete, as shown in Fig. 2. To estimate the interferometric transfer function of the instrument, we used a number of calibrators taken mainly from the Bordé et al. (2002) catalogue, which is an adaptation of the Cohen et al. (1999) catalogue for interferometric observations. The observations of these stars were used to estimate the point source response of the interferometer immediately before or after the Achernar observations. The raw data processing was achieved using the wavelet-based automated data reduction pipeline of VINCI (Kervella et al., 2004). This resulted in a total of 99 squared visibility measurements in the K band, and 19 in the H band, with their associated statistical and calibration uncertainties. The complete list of these visibility measurements can be found in Kervella & Domiciano de Souza (2006).

4. Modeling: from the star to the envelope

In order to define a plausible model for the light distribution of Achernar, we considered the shape of the polar and equatorial visibility functions. The orientation of the minor axis of Achernar on the plane of the sky relative to the North was obtained by D03 using a subset of the data available today. They obtained an orientation of the minor axis of Achernar (assumed to be the polar axis) of $\alpha_0 = 39 \pm 1°$ (counted from North towards East).

As shown in Fig. 3 (left), it appears that the distribution of the measured visibilities in the polar direction (between 10° and 70°) does not follow that of a uniform disk: there is a clear deficit of visibility at low spatial frequencies, indicative of a diffuse, resolved component.

The shape of the equatorial visibility function can be evaluated by restricting our sample to the visibility measurements obtained in the azimuth range 100-160°. Figure 3 (right) shows the distribution of squared visibilities observed in this azimuth range as a function of the spatial frequency. In this case, the fit of a simple uniform disk model with $\theta_{\rm UD} = 2.38$ mas produces satisfactory results with a reduced χ^2 of only 0.6. In this case, we conclude that we do not detect any significant diffuse envelope along the equatorial

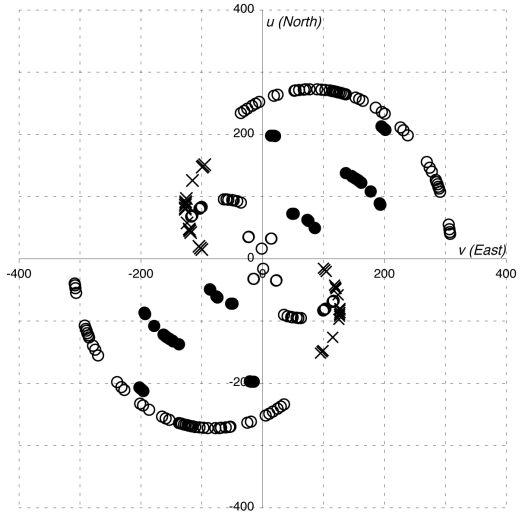

Fig. 2. Coverage of the (u,v) plane for the VINCI observations of Achernar. The units of both axes are cycles/arcsec. The open circles represent siderostat observations in K, the solid dots represent UT data in K, and the crosses are H band observations obtained with the siderostats.

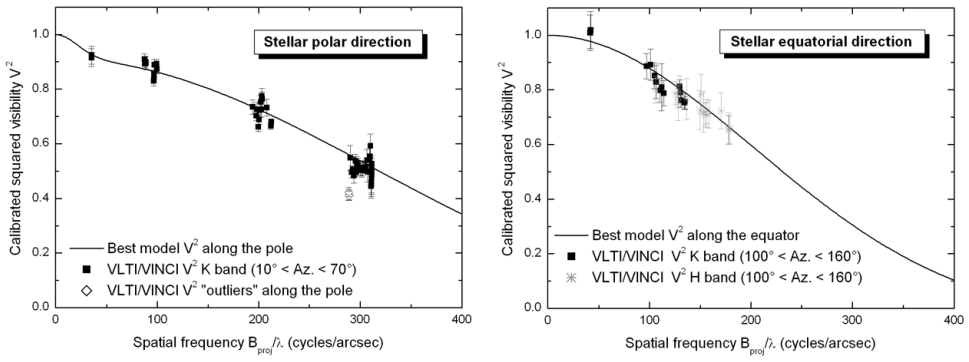

Fig. 3. *Left:* Squared visibilities V^2 measured on Achernar around the polar direction. *Right:* V^2 corresponding to projected baseline azimuth angles around the equatorial direction. The solid squares and crosses represent K and H band data, respectively. The solid curves represent theoretical V^2 along the pole (left) and the equator (right) obtained from the fit of an ellipse+CSE model (see text).

plane of the star.

So we considered three models of increasing complexity to fit the VINCI visibilities:

– a uniform disk model (usually correct for a normal star),
– a uniform ellipse (reasonable approximation of a fast rotating star without an envelope),
– a uniform ellipse + 2D gaussian ellipsoid (representing a CSE).

These visibility models present the advantage of having purely analytical expressions, that can be found in Kervella & Domiciano de Souza (2006). Fig. 4 shows the residuals of the best fits for the three models. From these figures and the reduced χ^2 of each fit, the model including a CSE stands out as the best description of the data. From the best-

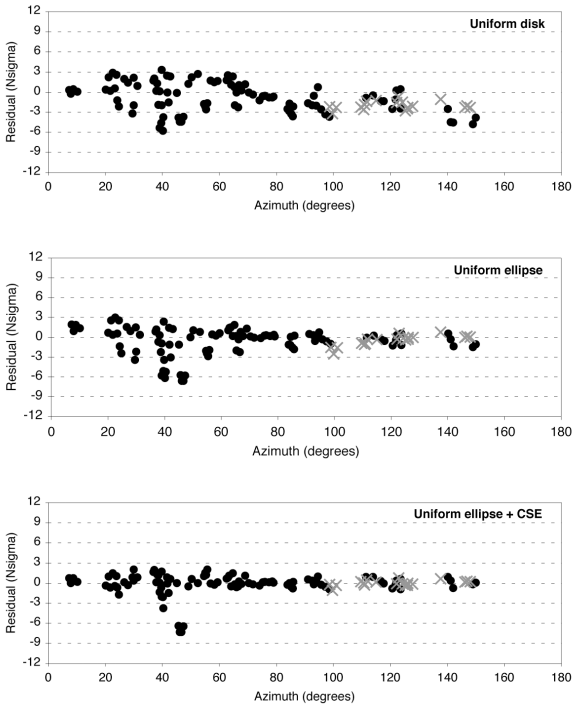

Fig. 4. Residuals of the fit of three visibility models fitted to the visibilities measured on Achernar, as a function of the azimuth angle of the projected baseline.

fit values of the free parameters, it appears that the envelope of Achernar is elongated along the polar direction of the star. A graphical representation of the star and its polar envelope based on the best-fit parameters is presented in Fig. 5. This figure is not a true image of the star, but only the representation of the best-fit light distribution with the a priori hypothesis that the star can be described by our ellipse+CSE model.

5. The winds of Achernar

What could explain the presence of such an elongated envelope in the direction of the poles of Achernar ? From the measured flattening ratio of the photosphere, the polar temperature of Achernar could be higher than 20 000 K. In this context, the radiation pressure reaches very high values. As was demonstrated in the case of the luminous blue variable star η Carinae (Van Boekel et al., 2003), a stellar wind ejected from the poles can have a detectable signature in the interferometric visibilities in the near infrared. In the case of of α Arae, another Be star similar to Achernar (rotation velocity, spectral type), recent AMBER observations (Meilland et al., 2006) also showed that an elongated polar wind should be included in the model together with a thin disk in order to explain the near-IR visibilities. Although the central stars are similar, one important difference is that α Arae presented hydrogen lines in strong emission during the interferometric observations, while they were absent from the spectrum of Achernar. Both stars show

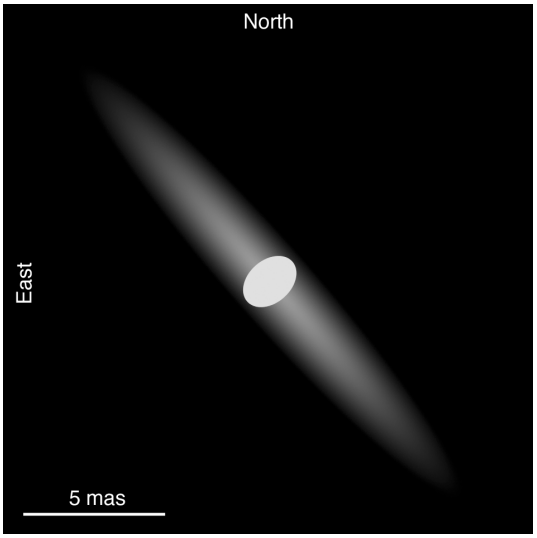

Fig. 5. Model fitted to the VINCI observations of Achernar. Note that this is *not* an image of the star.

an elongated polar wind responsible for a free-free and free-bound near-IR continuum emission, while only one of them (α Arae) shows a dense equatorial disk (resolved by VLTI/AMBER) where hydrogen emission lines are formed.

6. Fast rotating stars galore

Rapid rotation and gravity darkening seem to be important keys to explaining the two-component CSE of Be stars: a dense and low radial velocity equatorial envelope and a rarefied low mass-loss and fast polar wind. This standard picture of a two-component CSE is strengthened by the recent results obtained on α Ara and Achernar, and is the subject of an active observational and theoretical research. Recently, the rotational flattening effect was observed in several lower mass, rapidly rotating stars thanks to interferometric observations: Altair (Van Belle et al., 2001; Ohishi, Nordgren & Hutter, 2004; Domiciano de Souza et al., 2005; Peterson et al., 2006a), Regulus (McAlister et al., 2005), Alderamin (Van Belle et al., 2006) and Vega (Aufdenberg et al., 2006; Peterson et al., 2006b). These stars represent very favorable targets for interferometric imaging, as they present non-axisymetric light distributions due to their brighter polar caps. The search for evidence of the polar winds and disks of these moderately active stars (usually not emitting in the Hα line) requires high accuracy measurements, but is within reach of modern interferometric instruments.

References

Aufdenberg, J. P., Mérand, A., Coudé du Foresto, V., et al. 2006, ApJ, 645, 664, erratum ApJ, 651, 617

Balona, L. A., Engelbrecht, C. A., & Marang, F. 1987, MNRAS, 227, 123

Berger, J.-P., Haguenauer, P., et al. 2001, A&A, 376, 31

Bordé, P., Coudé du Foresto, V., Chagnon, G., Perrin, G., 2002, A&A, 393, 183
Chauville, J., Zorec, J., Ballereau, D., et al. 2001, A&A, 378, 861
Cohen, M., Walker, R. G., et al. 1999, AJ, 117, 1864
Damineli Neto, A., & de Freitas-Pacheco, J. A. 1982, MNRAS, 198, 659
Domiciano de Souza, A., Kervella, P., Jankov, S., et al. 2003, A&A, 407, L47
Domiciano de Souza, A., Kervella, P., Jankov, S., et al. 2005, A&A, 442, 567
Dougherty, S. M., & Taylor, A. R. 1992, Nature, 359, 808
Gehrz, R. D., Hackwell, J. A., & Jones, T. W. 1974, ApJ, 191, 675
Kervella, P., Coudé du Foresto, V., Glindemann, A., Hofmann, R. 2000, Proc. SPIE, 4006, 31
Kervella, P., Gitton, Ph., Ségransan, D., et al. 2003, Proc. SPIE, 4838, 858
Kervella, P., Ségransan, D. & Coudé du Foresto, V. 2004, A&A, 425, 1161
Kervella, P., & Domiciano de Souza, A. 2006, A&A, 453, 1059
Lebouquin, J.-B., Rousselet-Perraut, K., Kern, P., et al. 2004, A&A, 424, 719
Lebouquin, J.-B., Labeye, P., Malbet, F., et al. 2006, A&A, 450, 1259
McAlister, H. A., ten Brummelaar, T. A., Gies, D. R, et al. 2005, ApJ, 628, 439
Meilland, A., Stee, Ph., Vannier, M., Millour, F., Domiciano de Souza, A., et al. 2006, A&A, in press
Ohishi, N., Nordgren, T. E., & Hutter, D. J. 2004, ApJ, 612, 463
Peterson, D. M., Hummel, C. A., Pauls, T. A., et al. 2006, ApJ, 636, 1087
Peterson, D. M., Hummel, C. A., Pauls, T. A., et al. 2006, Nature, 440, 896
Quirrenbach, A., et al. 1997, ApJ, 479, 477
Slettebak, A. 1982, ApJS, 50, 55
Stee, Ph., de Araujo, F. X., Vakili, F., et al. 1995, A&A, 300, 219
Tycner, C., Lester, J. B., Hajian, A. R., et al. 2005, ApJ, 624, 359
Van Belle, G. T., Ciardi, D. R., Thompson, R. R., Akeson, R. L., & Lada, E. A. 2001, ApJ, 559, 1155
Van Belle, G. T., Ciardi, D. R., ten Brummelaar, T., et al. 2006, ApJ, 637, 494
Van Boekel, R., Kervella, P., Schöller, M., et al. 2003, A&A, 410, 37
Vinicius, M. M. F., Zorec, J., Leister, N. V., & Levenhagen, R. S. 2006, A&A, 446, 643
von Zeipel, H. 1924, MNRAS 84, 665
Waters, L. B. F. M., Cote, J., & Lamers, H. J. G. L. M. 1987, A&A, 185, 206